Effective Temperatures of a Driven System Near Jamming

Ian K. Ono[1], Corey S. O'Hern[1,2], Stephen A. Langer[3], Andrea J. Liu[1], and Sidney R. Nagel[2]
[1] *Department of Chemistry and Biochemistry, University of California, Los Angeles, CA 90095*
[2] *James Franck Institute, The University of Chicago, Chicago, IL 60637*
[3] *Information Technology Laboratory, NIST, Gaithersburg, MD 20899*
(Received:)

Fluctuations in a model of a sheared, zero-temperature foam are studied numerically. Five different quantities that reduce to the true temperature in an equilibrium thermal system are calculated. All five have the same shear-rate dependence, and three have the same value. Near the onset of jamming, the relaxation time is the same function of these three temperatures in the sheared system as of the true temperature in an unsheared system. These results imply that statistical mechanics is useful for the system and provide strong support for the concept of jamming.

83.80.Iz, 82.70.-y, 64.70.Pf

Statistical mechanics describes the connection between microscopic properties and collective many-body properties in systems in thermal equilibrium. There is no equivalent formalism for driven, athermal systems. Nonetheless, recent phenomenological approaches [1] that assume thermal behavior are surprisingly successful in describing driven glassy materials such as sheared foam. Foam is a dense packing of bubbles in a small amount of liquid, and is athermal because the thermal energy is much smaller than the typical energy barrier for bubbles to change their relative positions [2]. As a result, quiescent foam is *jammed* [2]; it is disordered and has a yield stress. If foam is steadily sheared, however, it is pushed over energy barriers and flows as different bubble packings are explored. However, it is unclear if this degree of ergodicity is enough to lead to thermal behavior.

In this Letter, we test the assumption that a sheared foam can be modeled as a thermal system with a temperature that depends on shear rate. We conduct numerical simulations of a simple model of sheared foam and measure five quantities that all reduce to the true temperature in a thermal system. Although these quantities must all have the same value in an equilibrium thermal system, there is no guarantee that they should be the same in the steadily-sheared model foam. Remarkably, three of the effective temperatures are the same and all five have the same shear-rate dependence. Our results for four of the effective temperatures are shown as a function of shear rate in Fig. 1 for two different size distributions of the bubbles. In a companion paper, Berthier and Barrat reach similar conclusions for a sheared thermal system [3]. These results suggest that statistical mechanics is indeed useful for describing driven jamming systems.

Our bubble dynamics (BD) simulations are carried out in two dimensions on Durian's model of foam [4]. The bubbles are circles with diameters assigned from one of two different diameter distributions. The first (polydisperse) distribution is flat from 0.2 to 1.8 times the average bubble diameter and is zero otherwise. The second (bidisperse) distribution consists of equal numbers of small and large bubbles of diameter ratio 1.4. Pairs of bubbles only interact, via a repulsive spring, when they overlap; this approximates the energy cost of bubble deformation [4]. There is also a frictional force proportional to the velocity difference between a bubble and the average flow at its position. The system is fully periodic, with flow in the $\hat{x}$ direction and a shear gradient in the $\hat{y}$ direction imposed using the Lees-Edwards boundary condition [5].

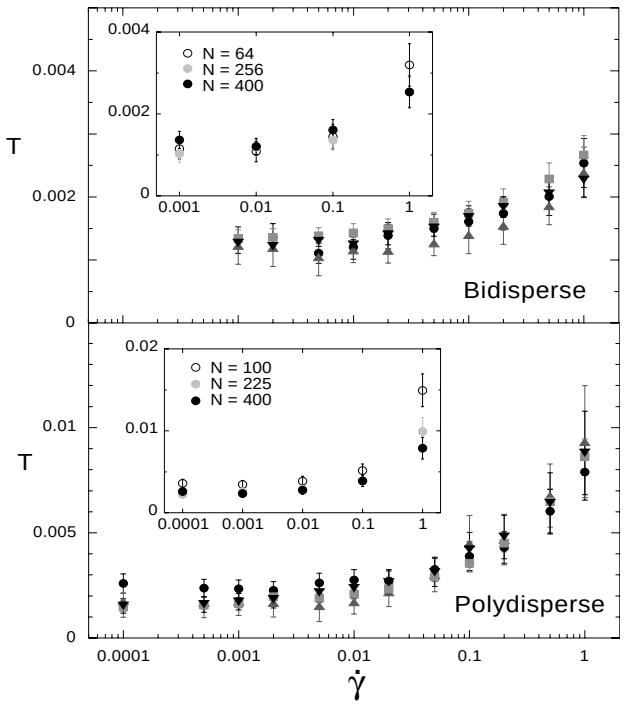

FIG. 1. Four effective temperatures, T_p (circles), T_{xy} (upward triangles), T_E (squares) and T_f (downward triangles) calculated as a function of shear rate. T_f has been rescaled by 4 and 2.7 for the polydisperse and bidisperse systems, respectively, to collapse on the others. Insets: T_p vs. $\dot{\gamma}$ for different system sizes.

We scale lengths by the average diameter d, energies by kd^2 where k is the spring constant, and time scales by $\tau_0 = b/k$, where b is the friction coefficient. Thus, the dimensionless shear rate $\dot{\gamma}$ is the Deborah number. Unless otherwise specified, the systems contain $N = 400$ bubbles at an area fraction of $\phi = 0.9$ (well above random close-packing at 0.84). Averages are typically taken over time snapshots separated by 0.1 in strain over a total strain of 10 for 100 (polydisperse) or 2 (bidisperse) different initial configurations.

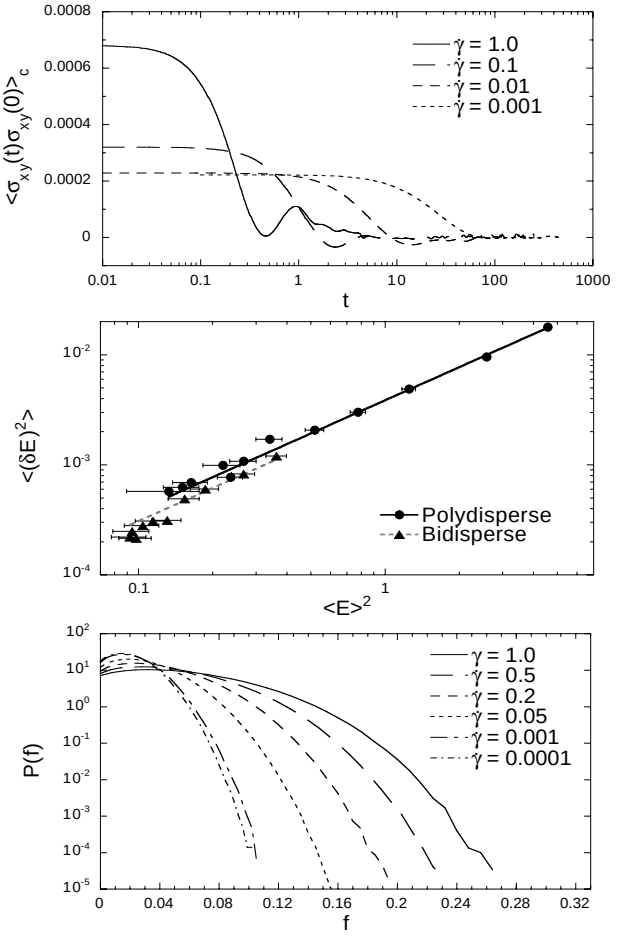

FIG. 2. (a) Shear stress autocorrelation functions at different shear rates for the polydisperse system (see Def. 2). (b) Variance of energy fluctuations plotted against average energy squared (Def. 3). The lines are fits to $\langle(\delta E)^2\rangle = m\langle E\rangle^2$, where $m = 3.9 \times 10^{-3}$ (polydisperse). (c) Force distributions $P(f)$ at different shear rates for the polydisperse system. The tail of $P(f)$ is fitted to a Gaussian centered at zero to obtain the effective temperature T_f (Def. 4).

Three of the 5 calculated effective temperatures are based on linear response relations or fluctuation-dissipation relations. Similar definitions have been used to characterize non-equilibrium systems in the contexts of weak turbulence [6], aging of glassy systems [7], granular packings [8,9] and sheared aging systems [2,10]; such effective temperatures can control the direction of heat flow and thus play the role of temperature in the thermodynamical sense in certain nonequilibrium systems with small energy flows [11].

Definition 1: pressure fluctuations. In an equilibrium system at fixed N, T and area A, the variance of the pressure is given by [5]

$$\langle p\rangle + \frac{\langle x\rangle}{A} - \beta_T^{-1} = \frac{A}{T}\langle(\delta p^2)\rangle \tag{1}$$

where $\beta_T^{-1} \equiv -A(\partial\langle p\rangle/\partial A)_T$ is the inverse isothermal compressibility, A is the area of the system, p is the pressure, x is the hyper-virial [5], and the Boltzmann constant is unity. In our driven, athermal system we thus define

$$T_p = \frac{A\langle(\delta p^2)\rangle}{\langle p\rangle + \frac{\langle x\rangle}{A} - \beta_T^{-1}}, \tag{2}$$

so that T_p reduces to the true temperature in an equilibrium thermal system. To measure the compressibility, we perturb the system area A and measure the resulting value of $\langle p\rangle$ during shear to calculate the derivative. In simulations of a quiescent system in thermal equilibrium with the same potential and polydispersity, we find that with comparable statistics, Eq. 1 yields results within 5% of the simulation temperature.

Definition 2: shear stress fluctuations. The viscosity of an equilibrium system is related to the integral over the shear stress autocorrelation function [5]:

$$\eta = \frac{A}{T}\int_0^\infty dt\langle\sigma_{xy}(t)\sigma_{xy}(0)\rangle_c \tag{3}$$

Again, we use Eq. 3 to define T_{xy}, calculating the steady-state shear viscosity from $\eta = \langle\sigma_{xy}\rangle/\dot{\gamma}$. The stress autocorrelation function is shown for several different shear rates in Fig. 2(a). With decreasing $\dot{\gamma}$, the correlation time increases approximately linearly, while the variance $\langle(\delta\sigma_{xy})^2\rangle$ decreases and then saturates.

Definition 3: energy fluctuations. The constant-volume heat capacity of an equilibrium system is related to energy fluctuations:

$$\frac{d\langle E\rangle}{dT} = \frac{\langle(\delta E)^2\rangle}{T^2}. \tag{4}$$

This can be rearranged and integrated on both sides to provide a definition of T [8]. To calculate T_E we must extract the relation between the variance of the energy fluctuations, $\langle(\delta E)^2\rangle$, and the average energy, $\langle E\rangle$. The results are shown in Fig. 2(b). We find that the variance scales as the square of the average energy, as shown by the line-fits to the data. The fits imply that $\langle E\rangle \propto T_E$, as can be seen by substitution into Eq. 4. In fact, we find $\langle E\rangle = 0.64NT_E$ for the polydisperse system and $\langle E\rangle = 0.56NT_E$ for the bidisperse system, where N is the number of bubbles in our two-dimensional system.

These results resemble equipartition, except that the coefficient of NT is not unity. Our potential is a harmonic repulsion with finite range, so equipartition is not exact.

Definition 4: force distribution. The temperature can be extracted from the tail of the distribution of interparticle normal forces $P(f)$ [13]. The force distribution is directly related to the pair correlation function $g(r) \equiv \exp(-\beta u(r))y(r)$ in a system with a pair potential $u(r)$. For r sufficiently small, the exponential term is a much stronger function of r (and hence of f) than $y(r)$. As a result, the tail of $P(f)$ depends on the interparticle potential and the temperature:

$$P(f) \approx \exp(-f^2/2T). \tag{5}$$

We fit the tail to extract T_f. Eq. 5 applies only to a monodisperse system. For a bidisperse system, we measure the distribution for small particles interacting with small particles only. For the polydisperse case, however, we use the force distribution for all particles (Fig. 2(c)). From MD simulations of an equilibrium system with the same potential, we have verified that this assumption should lead to no more than a 30% error in the computed T_f.

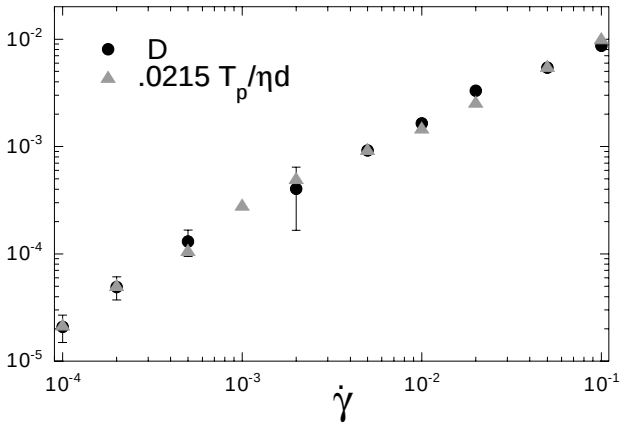

FIG. 3. The Stokes-Einstein relation. The circles represent the diffusion constant D, measured by integrating the velocity autocorrelation function. The triangles represent $T_p/C\eta d$, where C is a constant chosen to obtain the best fit with D.

Definition 5: Stokes-Einstein relation. In equilibrium, the diffusion constant D satisfies

$$D = \frac{T}{C\eta d}, \tag{6}$$

where C depends on system size in two dimensions. Thus, Eq. 6 defines a temperature T_D up to an unknown constant. Here we use fixed boundary conditions in the y-direction [12]. We measure D in the y-direction in two different ways and find good agreement: we integrate the velocity autocorrelation function, and we measure the displacement distribution as a function of time from an initial starting position. It is difficult to extract T_D because D and η vary by several orders of magnitude over the range of $\dot\gamma$ studied, while their product varies by less than an order of magnitude and has a lot of scatter and large error bars. This definition is therefore most useful as a consistency check: we use T_p from Def. 1 and vary C to obtain the best agreement between the left and right sides of Eq. 6. Fig. 3 shows that the Stokes-Einstein relation is indeed obeyed.

Our results for the other four effective temperatures (Defs. 1-4) are plotted in Fig. 1. The insets show that the temperatures do not depend on system size for N sufficiently large. All the temperatures have the same shear rate dependence over 4 decades of $\dot\gamma$. Since we do not have a first-principles calculation of C, the magnitude of T_D is not known. However, T_f is different in magnitude (but not in $\dot\gamma$-dependence) from the remaining three. One possible reason for the discrepancy is that T_f measures the properties of the *tail* of $P(f)$, while T_p, T_{xy} and T_E measure fluctuations around average quantities. This suggests that the underlying probability distribution may not be a Boltzmann distribution.

Fig. 1 suggests that the effective temperatures approach nonzero constants $T^0_{\rm eff}$ in the limit $\dot\gamma \to 0$. In fact, this is expected from their definitions. As long as bubbles overlap as $\dot\gamma \to 0$, the force distribution $P(f)$ is nonzero for $f > 0$, and yields $T^0_f > 0$. The other temperatures should also be nonzero; in the zero shear rate limit, the angular brackets indicate configurational averages rather than time averages. This suggests an interpretation of the limiting value; $T^0_{\rm eff}$ should correspond to the glass transition temperature T_g. By shearing the system and calculating averages over times long compared to the relaxation time (which scales as $1/\dot\gamma$), we are demanding that the system is ergodic. Therefore, the only temperatures accessible to us are above T_g.

We have checked the interpretation of $T^0_{\rm eff}$ as T_g by conducting equilibrium molecular dynamics (MD) simulations on a system with the same interaction potential, packing fraction, and size distribution (bidisperse) as in our bubble dynamics (BD) runs. It has been proposed that jamming systems such as this one can be described by a phase diagram [14], sketched in the inset to Fig. 4. This diagram shows that jamming occurs as T is lowered, the packing fraction ϕ is raised, or the applied shear stress σ_{xy} is lowered, and has been shown to be a useful way to represent experimental data [15]. The BD results in Fig. 1 correspond to the trajectory marked "BD" in the inset to Fig. 4. In the MD simulations, we have removed the frictional term from the equations of motion and added the inertial term and true temperature so as to approach jamming along the trajectory marked "MD." In Fig. 4, we show the results for the relaxation time τ as a function of T from MD and BD, at two different packing fractions, $\phi = 0.85$ and $\phi = 0.90$. The lower packing fraction is just above random close-packing. In MD, we measure τ from the decay of the intermediate

scattering function [16]. In BD, we plot $\tau = c/\dot{\gamma}$, where c is a constant chosen to best fit the MD data [17], as a function of T_E.

Fig. 4 shows that the dynamics are the *same* for a system approaching jamming by two different trajectories: decreasing T and decreasing $\dot{\gamma}$ (or equivalently, decreasing $\langle\sigma_{xy}\rangle$). Thus, T_g from MD at zero applied shear is the same as $T^0_{\rm eff}$ from BD. A similar result was found previously for a sheared thermal Lennard-Jones mixture [10]. Fig. 4 also shows that the *functional form* of the slowing down of the dynamics is the same along both trajectories for low T. This is consistent with previous work showing that the dynamics of the sheared model foam can be described by a Vogel-Fulcher form [12]. An attempt to collapse the data for the two different ϕ using an Angell fragility plot [18] shows that the fragility depends on packing fraction.

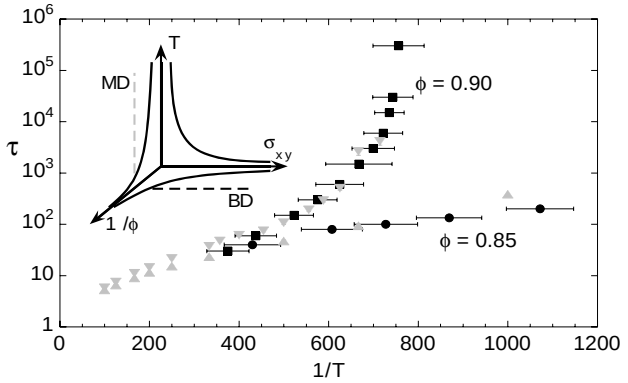

FIG. 4. An Arrhenius plot of the relaxation time as a function of temperature from MD (gray symbols) and BD (black symbols) simulations at two different packing fractions, $\phi = 0.85$ and $\phi = 0.90$. Inset: the jamming phase diagram. Our bubble dynamics simulations follow the trajectory marked BD, while our molecular dynamics simulations follow the trajectory marked MD.

The results in Fig. 4 provide confirmation of the idea underlying the jamming phase diagram, namely, that the jammed region controls the behavior nearby so the dynamics should not depend on the direction along which the jammed region is approached [14,2]. It also suggests that one can collapse the $\sigma-$axis onto the $T-$axis using $T_{\rm eff}$, and that a system will jam once fluctuations, whether thermal or shear-induced, are sufficiently small.

Our main finding that 5 different effective temperatures have the same $\dot{\gamma}$ dependence raises the need for a criterion for when the concept of effective temperature might be useful. We suggest such a criterion based on the idea underlying the fluctuation-dissipation relation. An analogous concept applies to a steady-state driven system, because the average power supplied to the system must be balanced by the average power dissipated. The power can be dissipated in two ways–by the average flow and by fluctuations around the average flow. We speculate that the concept of effective temperature is useful if nearly all the power supplied by the driving force is dissipated by fluctuations. In the model studied here, all of the power is, by construction, dissipated by fluctuations–the frictional force is proportional to the difference between the velocity of a bubble and the average shear. In systems in the stick-slip regime near jamming, fluctuations typically are large compared to the average flow [2]. This suggests that the concept of effective temperature should be useful for *any* system near the onset of jamming.

We are grateful to B. C. H. Ng for carrying out some of the runs. We thank D. J. Durian and C. M. Marques for instructive discussions. This work was supported by NSF-DMR-0087349 (IKO,CSOH,AJL) and NSF-DMR-9722646 (CSOH,SRN).

[1] P. Sollich, F. Lequeux, P. Hébraud, M. E. Cates, Phys. Rev. Lett. **78**, 2020 (1997); P. Hébraud, F. Lequeux, Phys. Rev. Lett. **81**, 2934 (1998); C. Derec, A. Ajdari, F. Lequeux, Eur. Phys. J. E **4**, 355 (2001).

[2] See *Jamming and Rheology* ed. A. J. Liu and S. R. Nagel (Taylor and Francis, New York, 2001), and references therein.

[3] L. Berthier and J.-L. Barrat, submitted to Phys. Rev. Lett.

[4] D. J. Durian, Phys. Rev. Lett. **75**, 4780 (1995); Phys. Rev. E **55**, 1739 (1997).

[5] M. P. Allen and D. J. Tildesley, *Computer Simulation of Liquids* (Oxford University Press, New York, 1987).

[6] P. C. Hohenberg and B. I. Shraiman, Physica D **37**, 109 (1989).

[7] L. F. Cugliandolo and J. Kurchan, Phys. Rev. Lett. **71**, 173 (1993).

[8] E. R. Nowak, J. B. Knight, E. Ben-Naim, H. M. Jaeger, S. R. Nagel, Phys. Rev. E **57**, 1971 (1998).

[9] H. Makse and J. Kurchan, cond-mat 0107163.

[10] J.-L. Barrat and L. Berthier, Phys. Rev. E **63**, 012503 (2001).

[11] L. F. Cugliandolo, J. Kurchan, L. Peliti, Phys. Rev. E **55**, 3898 (1997).

[12] S. A. Langer and A. J. Liu, Europhys. Lett. **49**, 68 (2000).

[13] C. S. O'Hern, S. A. Langer, A. J. Liu, S. R. Nagel, Phys. Rev. Lett. **86**, 111 (2001).

[14] A. J. Liu and S. R. Nagel, Nature **396** N6706, 21 (1998).

[15] V. Trappe, V. Prasad, L. Cipelletti, P. N. Segre, D. A. Weitz, Nature **411**, 772 (2001).

[16] W. Kob and H. C. Andersen, Phys. Rev. E **52**, 4134 (1995).

[17] The time scales in the BD and MD simulations have different units because there is a friction coefficient in BD and a particle mass in MD, so we are free to choose a scale factor for τ.

[18] C. A. Angell, J. Non-Cryst. Solids, **131-133**, 13 (1991).